USE OF COAXIAL-FIBER OPTICS AND PRISM-GRATING-PRISM ARRAYS IN AN EXCITATION-EMISSION MATRIX (EEM) FLUOROMETER FOR THE DETECTION OF POLYAROMATIC HYDROCARBONS

by

Diana M. Chávez

A thesis submitted to the Faculty of the University of Delaware in partial fulfillment of the requirements for the degree of Master of Science in Chemistry and Biochemistry

Spring 2018

© 2018 Diana M. Chávez
All Rights Reserved

USE OF COAXIAL-FIBER OPTICS AND PRISM-GRATING-PRISM ARRAYS IN AN EXCITATION-EMISSION MATRIX (EEM) FLUOROMETER FOR THE DETECTION OF POLYAROMATIC HYDROCARBONS

by

Diana M. Chávez

Approved: _____
Karl S. Booksh, Ph.D.
Professor in charge of thesis on behalf of the Advisory Committee

Approved: _____
Brian J. Bahnson, Ph.D.
Chair of the Department of Chemistry and Biochemistry

Approved: _____
George H. Watson, Ph.D.
Dean of the College of Arts and Sciences

Approved: _____
Ann L. Ardis, Ph.D.
Senior Vice Provost for Graduate and Professional Education

ACKNOWLEDGMENTS

Karl S. Booksh, Ph.D., for mentoring this work and for giving me the opportunity of growing up professionally.

Yoon-Chang Kim and James A. Jordan, for sharing their knowledge with me. Their experiences and advises were important to my research.

The friends and collaborators in the Booksh group for their help and support during my stay in Delaware, especially to my office mates Nicola Menegazzo, Bryon Herbert and Lauren Kegel.

This manuscript is dedicated to:

My mom Elena Castillo, for her unconditional support.

My children, Andrea, Camilo and Marcelo, for being my best motivation.

My husband, Juan Carlos, for being always by my side with his courage, love and patience.

TABLE OF CONTENTS

LIST OF TABLES v
LIST OF FIGURES vi
ABSTRACT vii

Chapter

1 POLYAROMATIC HYDROCARBONS AND EXCITATION EMISSION MATRIX SPECTROMETRY 1

1.1 Polyciclic Aromatic Hydrocarbons and their impact in human health 1
1.2 Excitation-emission matrix (EEM) fluorescence spectroscopy 3
1.3 Strategies to increase portability of EEM devices. 5

2 METHODOLOGY 7

2.1 Experiments with coaxial fiber 7
2.2 Experiments with cuvettes. 10

3 RESULTS AND DISCUSSION 13

3.1 Experiments with coaxial fiber 13
3.2 Evaluation of the equipment with cuvettes. 17

4 CONCLUSIONS 20

REFERENCES 21

LIST OF TABLES

Table 1. Maximum contaminant levels (MCM) for selected PAHs by EPA 2

LIST OF FIGURES

Figure 1. Examples of polyaromatic hydrocarbons (PAH).[4] 2

Figure 2. Scheme showing the electronic transitions from excitation and emission. 4

Figure 3. Scheme showing the formation of a excitation-emission spectrum 4

Figure 4. Setup for excitation-emission matrix (EEM) spectroscopy. 5

Figure 5. Picture of fiber optic EEM fluorometer 8

Figure 6. Twelve coaxial fibers held in the excitation chuck. 9

Figure 7. Picture of the prototype EEM fluorometer with its components indicated. 11

Figure 8. Overlapping acceptance cones for EEM components of the coaxial fiber. 13

Figure 9. Emission spectrograph/CCD images of halogen lamp 14

Figure 10. Reflected white light collected from the coaxial fiber optic 16

Figure 11. EEM spectra images of two PAHs and their mixture 17

Figure 12. Calibration spectra. 18

Figure 13. Representative EEM spectra for pure samples of 3 PAHs and a mixture. 19

Figure 14. Reconstructed spectra obtained from the PARAFAC analysis. 19

ABSTRACT

This work presents two strategies to improve the portability of an Excitation-Emission Matrix (EEM) fluorometer and its selectivity in the detection of polyaromatic hydrocarbons (PAHs). These organic compounds are of interest from an environmental point of view because they are persistent and small quantities are sufficient to be considered a threat to human health and environment. The first strategy is the replacement of a spectrograph by a prism-grating-prism (PGP or grism), which would facilitate portability. The second strategy is to use coaxial fibers to overcome the physical constrains to use two spectrographs. Both strategies are tested in this thesis, and the results show that each one of them presents advantages that are worth considering.

Chapter 1

POLYAROMATIC HYDROCARBONS AND EXCITATION EMISSION MATRIX SPECTROMETRY

Polyciclic Aromatic Hydrocarbons and their impact in human health.

One of the most dangerous groups of carcinogenic compounds is that of polycyclic aromatic hydrocarbons (PAHs). They are semi volatile organic compounds containing two or more fused aromatic rings (Fig. 1). PAHs are naturally found in oil and as product of spontaneous forest fires and volcanic emissions. However, the major sources of PAH are anthropogenic, i.e., they are the product of human activities such as incomplete combustion and pyrolysis of organic matter, such as coal, oil, wood, and fuels like diesel and petrol, as in petroleum spillage, incineration and industrial and municipal discharge. Once in the air, PAHs can be adsorbed onto smoke particles so they are transferred to several places, including the aquatic environment[1–3].

There are 16 PAHs recognized by the Environmental Protection Agency (EPA) as primary pollutants which include: naphthalene; acenaphtylene; acenaphthene; benzo(g,h,i)perylene; fluorene; phenanthrene; dibenzo(a,h)anthracene; ideno(1,2,3-c,d)pyrene; anthracene; benzo(a)pyrene; benz(a)anthracene; benzo(b)fluoranthene; benzo(j)fluoranthene; benzo(k)fluoranthene; chrysene; fluoranthene and pyrene.[4,5] These compounds are sufficiently dangerous to have extremely low permitted levels. According to EPA, for example, the limit of several PAHs in water is in the range of parts per billion (ppb). Table I shows maximum contaminants levels values in water according to U.S. Environmental Protection Agency for selected PAHs.

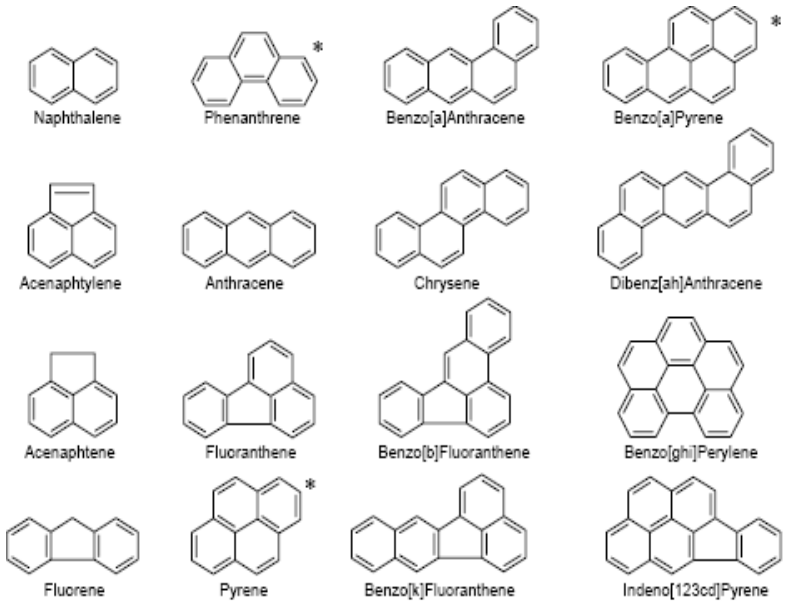

Figure 1. Examples of polyaromatic hydrocarbons (PAH).[4]

Table **1.** Maximum contaminant levels (MCM) for selected PAHs by EPA.[6,7]

PAH compound	MCL μg/L (ppb)
benz(a)anthracene	0.1
benzo(a)pyrene, benzo(b)fluoranthene, benzo(k)fluoranthene, chrysene	0.2
dibenz(a,h)anthracene	0.3
indenol(1,2,3-c,d)pyrene	0.4

This study will focus on the analysis of PAHs in water, where they are found as mixtures of various compounds. The challenge is to discern between different PAHs in this mixture, especially because they have similar electronic properties, which means that their signals using conventional spectroscopic techniques are strongly overlapped and cannot be deconvoluted. For example, conventional fluorescence spectra present fluorescence only within one spectral region and does not

provide enough data to distinguish between two or more closely related molecules. This disadvantage of a conventional fluorometer can be overcome by extending the dimensionality of the fluorescence measurements such as excitation-emission matrix (EEM) fluorescence spectroscopy[8,9]

Excitation-emission matrix (EEM) fluorescence spectroscopy

This technique, hereafter called EEM for simplicity, employs a light beam to irradiate the sample and certain wavelengths are absorbed and electronic transitions take place, resulting in an emission spectrum. Figure 2 shows a scheme of the processes involved at an electronic level and Fig. 3 shows a schematics of the image resulting from combining the information from emission and excitation. Due to its two-dimensional character, EEM spectroscopy offers an increased selectivity. Then, it is possible to identify individual components in a mixture of compounds, providing that the appropriate mathematical tools are available[1,10].

By collecting EEM spectra for several samples, the data becomes tri-dimensional. This "data cube" can be analyzed using advanced chemometric techniques, such as Parallel Factor analysis (PARAFAC). In PARAFAC, the data is deconvoluted and separated for a number of factors (components) present. Due to the multi-way nature of the data, the solution is unique [11,5].

The development of fluorescence spectroscopic instruments involves specification of system components including light sources, spectrometers, detectors, and associated elements, arranged in a fashion described as in Figure 4.

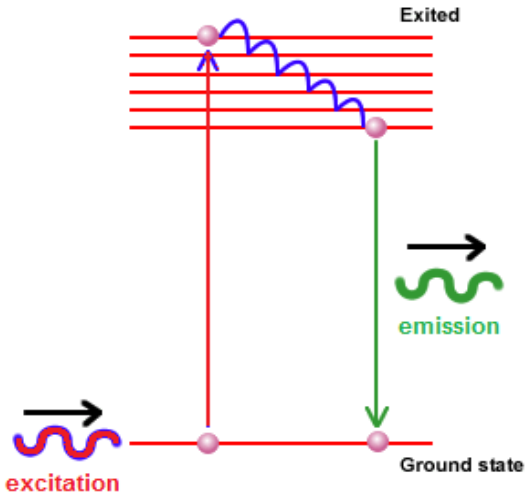

Figure 2. Scheme showing the electronic transitions from excitation and emission.

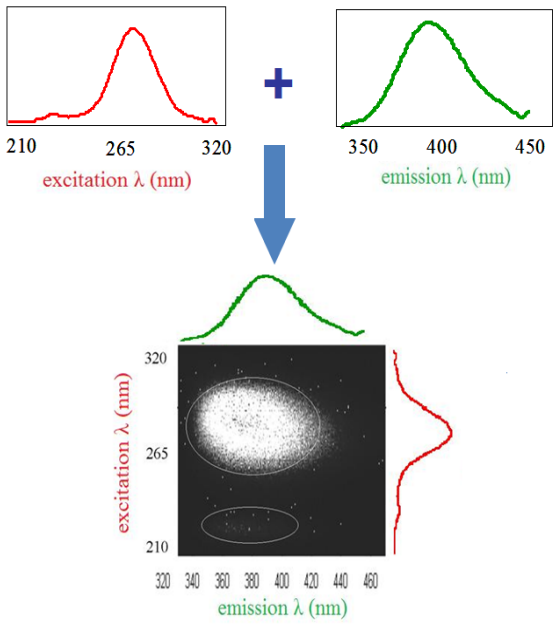

Figure 3. Scheme showing the formation of a excitation-emission spectrum

Strategies to increase portability of EEM devices.

Although the setup for EEM analysis shown in Fig. 4 is advantageous for analysis in the laboratory, portable devices based on this setup are not practical due to the large size of the components and the sensibility of the arrangements of components. This limits the applicability of the technique. For this reason, one of the goals of this thesis is to design a new EEM setup in which the second spectrograph (the one attached to the CCD camera) is replaced by an optical array prism-grating-prism (grism) of smaller dimensions. Grisms have been used previously in optical arrays due to the possibility of turning cameras into spectrographs, especially for astronomic measurements.[12,13]

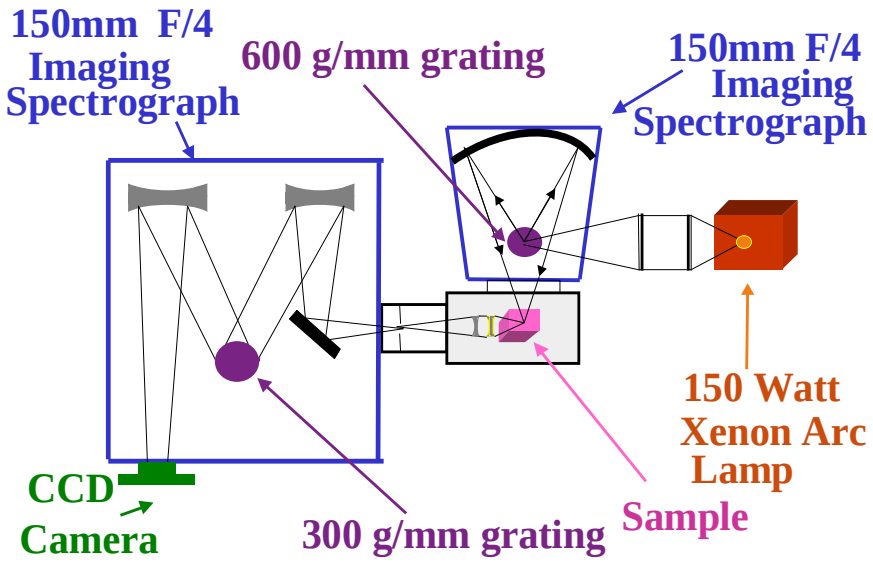

Figure 4. Setup for excitation-emission matrix (EEM) spectroscopy.

An even more fitted design for portability can be obtained by employing optical fiber probes, since they eliminate the physical constraints on the spectrometers and can allow in situ measurements without a loss of performance. Employing an array of coaxial optical fiber probes to simplify EEM fluorescence instrumentation is a novel design and application which is an additional goal in this work. Numerous single- and dual-fiber configurations have been employed for spectroscopic applications[14]. In a single-fiber probe, the fiber that delivers the light to the sample is also utilized for collection of the fluorescent signal. The overlap is complete and independent of the distance from the probe tip. However, the returning emitted/scattered light needs to be separated from the excitation light by an optical device such as an optical circulator or a dichroic beam splitter, which can result in interference problems[15]. Dual-fiber probes typically use one fiber to deliver the excitation lights and the other fiber to collect the signal that is generated by the sample. The efficiency of fiber-optic fluorescence probes depends on the spatial overlapping between the cone in which the excitation light propagates and the fluorescence collection cone[16]. Dual-fiber probes typically offer poor overlap between the excitation and collection cones, because they utilize separate fibers for excitation and collection and the symmetry axes of the corresponding cones do not coincide.

In the present study, we design and develop two strategies for improving the portability of EEM devices, one based on the use of a grism and the other on the use of coaxial fibers.

Chapter 2

METHODOLOGY

Experiments with coaxial fiber

As it was mentioned in the Introduction Section, usual models include two spectrographs (Fig. 4), which may be inefficient in terms of portability. The setup shown in Fig. 5 replaces one spectrograph with a prism-grating-prism (PGP) array (indicated by letters g and h in Fig. 5) and includes the array of optical fibers (c through e in Fig. 5). When only the PGP array was tested, the configuration changed to ensure that the light from the spectrograph (b) was aligned with the UV lenses (f) and the PGP array (g-h). The PGP parameters (distance between components and angles in prisms) were optimized using the FRED software (Photon Engineering, AZ). A capture of this software during optimization of the PGP parameters is shown in the inset of Fig. 5 (5.k). The excitation source in the EEM fluorometer was an Oriel® Apex Arc Lamp Source (75W Xe, Newport Corporation, Irvine, California). The Oriel MS125™ Spectrograph (Newport Corporation) with a ruled grating (600 l/mm of line density and 200 nm of blaze wavelength) served as the dispersion unit with a 180 nm – 500 nm excitation range. The emission spectrometer was based on the grism design and composed of two UV camera lenses [105 mm F/4 UV-Micro-Apo, (Coastal optical systems, West Palm Beach, Florida)], a wedge prism [2" of OD and 25 deg of wedge angle, (Mark optics incorporated, Santa Ana, California)], a UV transmission grating [1200 grooves/mm, (Thor Labs, Newton, Ney Jersey)], and a 8 x 8 mm CCD detector [iXonEM+ 855 EMCCD, (Andor Technology, Belfast, United Kingdom)].

The software used to collect spectroscopic data was Andor SOLIS for Imaging (Andor Technology, version 4.5.0.0). At the entrance portion to the emission spectrometer, the emission fibers are held in a column by an anodized aluminums plug, which is interfaced to this spectrometer for emission collection.

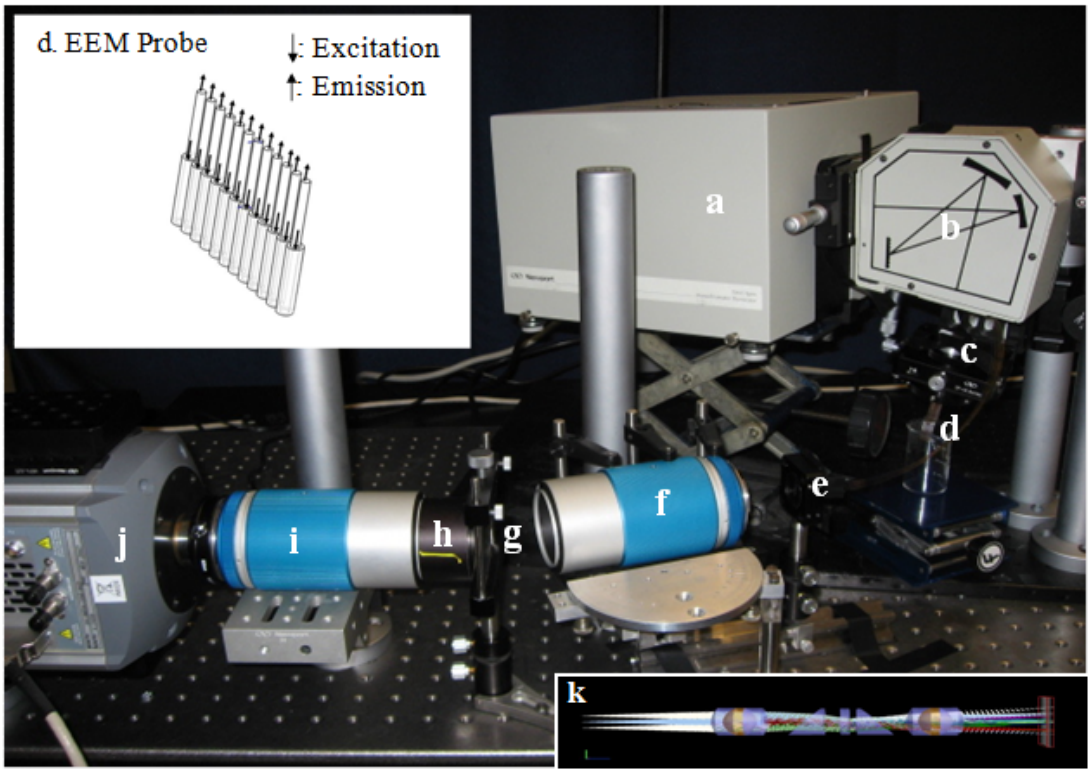

Figure 5. Picture of fiber optic EEM fluorometer. a) arc lamp source; b) spectrograph; c) excitation fibers holder; d) EEM probe; e) Emission fibers holder; f) UV lenses; g) Transmission grating; h) Wedge prism; i) UV lenses, j) CCD camera. The inset in the bottom (k) is a capture of the FRED program employed to computationally optimize the configuration of the prism-grating-prism array.

To construct the coaxial fiber array, a length of high OH, UV enhanced, silica/silica optical fiber with polyamide cladding (Polymicro Technologies, FVP/200/220/245) was inserted into a light guiding flexible fused silica capillary (Polymicro Technologies LTSP250/665). The inner fiber had a 200 μm diameter core, 10 m cladding and 7 mm polyamide buffer for a total outer diameter of approximately 245 μm. The capillary had a 250 μm inner diameter core and 625 μm outer diameter core. The net outer diameter was 645 μm with cladding and polyamide buffer. The optical fiber and capillary combination was chosen to maintain good overlap with of the excitation and collection cones.

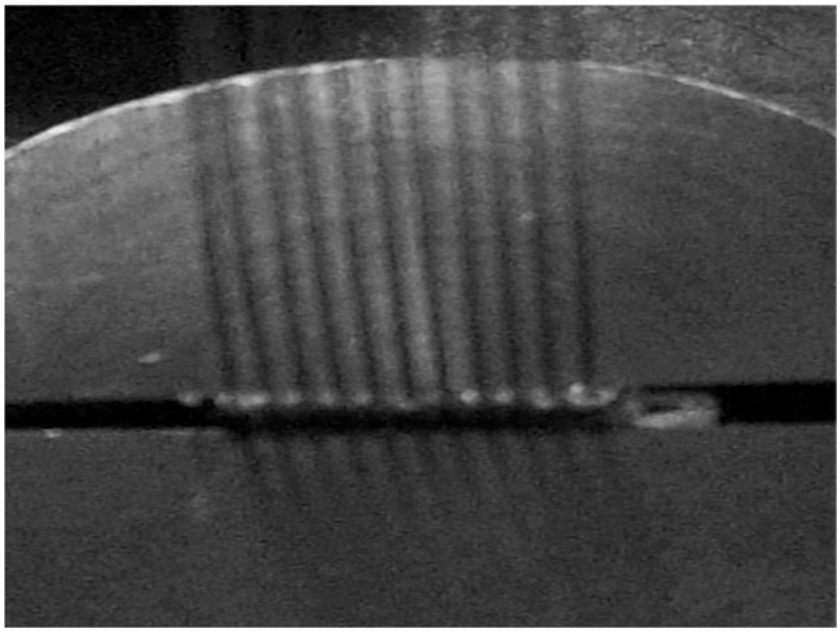

Figure 6. Twelve coaxial fibers held in the excitation chuck. The emission fibers are bent to exit the spectrograph through the side port. There is a little shadowing of the outer capillary by the inner fibers in this configuration but the center fibers are very out of focus when they shadow the outer capillary.

To interface the coaxial fiber array with the spectrometers, an anodized aluminum holder was fabricated (Figure 6). Twelve coaxial fibers were arranged in a linear array. The distal end of the array was polished flat with 1 μm lapping film. The outer capillaries were held at the exit slit of the excitation spectrograph. The inner fibers consequently enter the excitation spectrograph through the slit, exits through a hole drilled in the wall of the spectrograph and is then aligned along the entrance slit of the emission spectrograph. The array could be realigned with the outer capillary along the emission and inner along the excitation. However, it was found that greater signal-to-noise ratio (S/N) was realized with the more compact inner fiber array being imaged onto the CCD. That is to say, both the inner optical fiber and outer capillary are smaller than the putative focus of the emission spectrometer so there is no essential difference in spatial photon density entering either waveguide when placed at the excitation slit. However, the fiber core is 200 μm in diameter while the outer capillary is 625 μm in diameter. Thus, the same number of fluoresced photons strikes the CCD using either the core or cladding for collection. The main difference resides in that the core would be imaged across 25 pixel wide stripe of the detector while the capillary would be imaged across a 78 pixel wide stripe of the detector.

Experiments with cuvettes.

For this set of experiments the configuration of the equipment has changed. The excitation source, an Oriel® Apex Arc Lamp Source (75W Xe) and the Oriel MS125™ Spectrograph which served as the dispersion unit with are now in a vertical position. The emission spectrometer was based on the grism design and composed of two UV camera lenses (105 mm F/4 UV-Micro-Apo, Coastal optical systems), a

wedge prism (2" of OD and 25 deg of wedge angle, Mark optics incorporated), a UV transmission grating (1200 grooves/mm, Thorlabs), and a CCD detector (iXonEM+ 855 EMCCD, Andor). The software used to collect spectroscopic data was Andor SOLIS for imaging (version 4.5.0.0). The configuration set up is show in Figure 7.

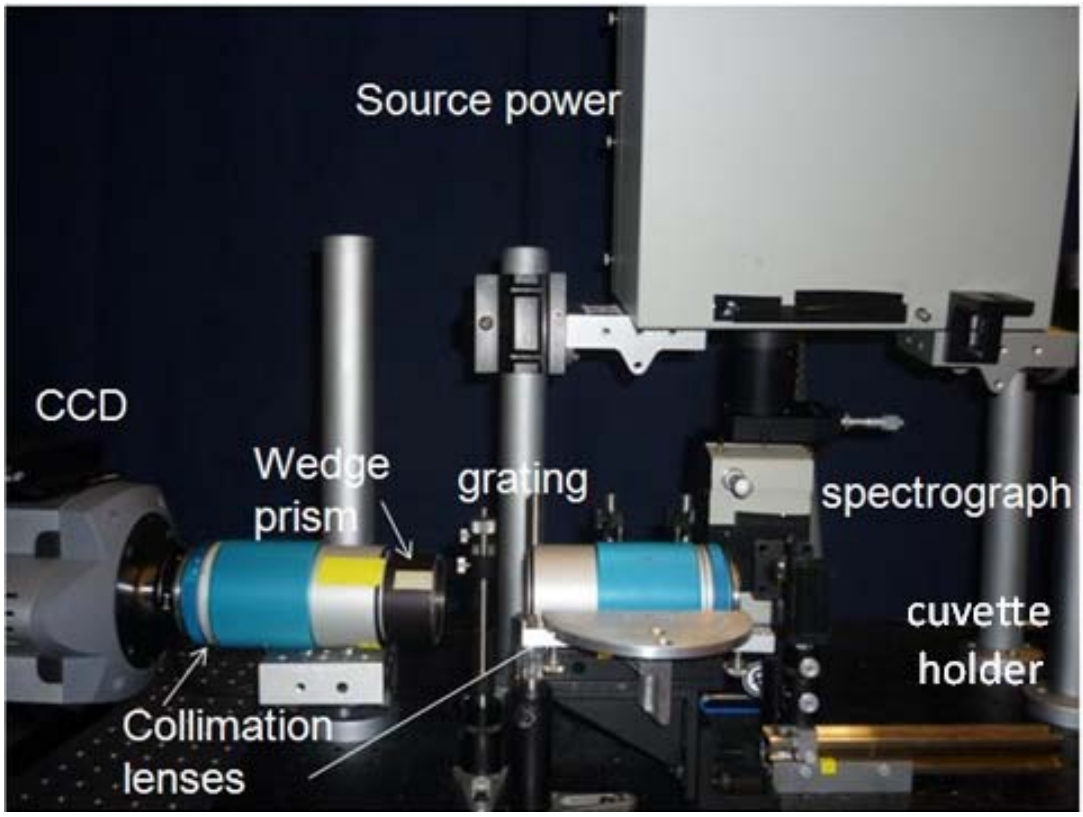

Figure 7. Picture of the prototype EEM fluorometer with its components indicated.

The initial experiments to obtain a portable EEM fluorometer were performed using rectangular fluorometer cells [10 mm path length, Spectrosil Quartz 170 to 2700nm Starna Cells Inc. (Atascadero, California)] for samples. A cuvette holder was designed to use the rectangular cells in which the emission response was expected to

occur in 90 degrees angle, for those consideration two continuous windows were opened and the other two closes. The holder was made of anodized aluminum, painted with a matte black paint and was constructed in the machine shop facilities.

Polycyclic aromatic hydrocarbons are organic compounds which are adsorb to the wall of the glassware due to the presence of silanol groups (SiOH) of the glass. In order to avoid mass loss in measurement and the decrease of the sensivity in our low sample concentrations, all the glassware used were previously silanizated using two processes: preparing the dimethylcholorosilane and using a commercialized dimethylcholorosilene solution[17].

Procedure for preparing the dimethylcholorosilane solution.

- In a chemical fume hood, add the dimethylcholorosilane solution (10% in toluene) to the glassware. Completely cover all the glassware with the solution.
- Incubate for 30 minutes at room temperature in the fume hood.
- Remove the silanizing solution.
- Rinse the glassware with toluene three times.
- Rinse the glassware with methanol three times.
- Dry glassware at room temperature (do not use an oven or heating mechanisms to avoid losing the calibration the volumetric glassware). Clean nitrogen can be added (Note: compressed air lines can contain oils, rust particles, etc.).

Chapter 3

RESULTS AND DISCUSSION

Experiments with coaxial fiber

Figure 8 shows an image of light launched down the optical fiber and capillary waveguides. At 1 cm from the coaxial fiber, there is near complete overlap of the inner fiber acceptance cone with the capillary acceptance cone.

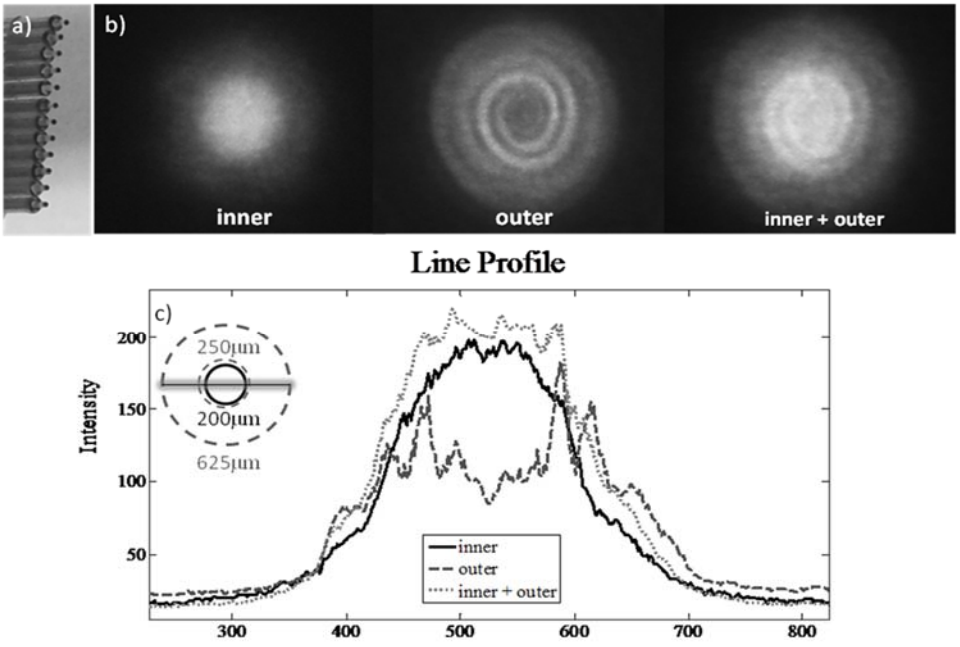

Figure 8. Overlapping acceptance cones for EEM components of the coaxial fiber. A) Image of the fiber array; B) Projected image of the optical profile 1 cm distant from the excitation and emission components of the coaxial array; and C) Line profiles along the center of the fibers showing overlap of the acceptance cones.

To demonstrate the separation of the fibers on the CCD and calibrate the emission spectrometer, broad spectrum white light (Figure 9a) and light from a Hg-Ar (HG-1, Ocean Optics) calibration lamp (Figure 9b) were launched down the capillary array, reflected off of a mirror and collected by the optical fibers. The pixel size of the CCD detector was 1002×1004 and it had 1002 pixels in the spectral direction and 1004 in the spatial direction. The dimensions of a pixel and an image area are 8 μm ×8 μm, and 8 mm × 8mm, respectively. The CCD is binned into twelve channels to detect the light from the twelve emission fibers of EEM probe. Each channel is composed of 26 – 30 rows of pixels, with fifty four to sixty one unused rows between channels to reduce the cross-talk due to charge blooming and spectrograph aberrations.

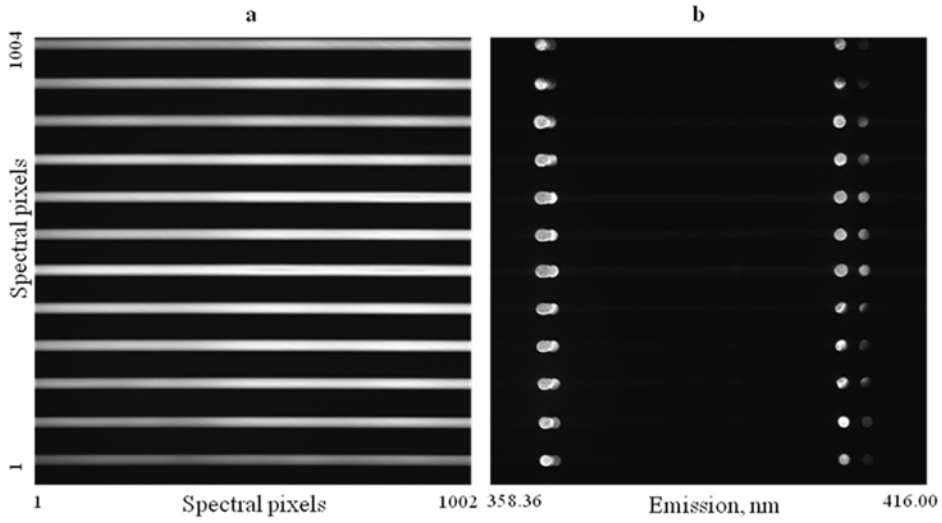

Figure 9. Emission spectrograph/CCD images of halogen lamp (a) and mercury calibration lamp (b) through 12 coaxial fibers for calibration of the emission spectrometer. Excellent separation between the fibers is realized.

The wavelength scale of the emission spectrometer was calibration from an image of the Hg-Ar lamp. The five spots at each fiber are correlated with the known wavelengths (365.02, 365.48, 366.33, 404.66, 407.78 nm) and a linear polynomial fit was calculated to translate pixel into wavelength. The equation for the fitted line is

$$\lambda em = 0.05758Pem+358.3, \quad (1)$$

Where λem is the emission wavelength increase in nm and Pem is pixel number increase for emission. The root mean square error (RMSE) of the calibration across the pixel range, 115 – 860 is 0.1018. The angles of wedge prism and collimated light from the UV camera lens were set for this test so that the CCD detects the horizontal emission wavelengths in the region of 358 nm to 416 nm.

The CCD images of reflected light from a mirror and Rayleigh scattering from a starch solution were employed to calibrate the excitation spectrometer (Figure 10a and 10b, respectively). In the Figure 10a, the intensities clearly peak in the centers of the fibers which enable high-accuracy spectral measurement. A linear polynomial fit of the centers is calculated to translate emission pixel number into excitation pixel number. Given that $\Delta\lambda em = \Delta\lambda ex$ for elastically scattered or reflected light, the calibration of the emission spectrometer can be employed to calibrate the excitation spectrometer. By way of a first order polynomial fit, the relationship between CCD pixel and excitation wavelength was found to be

$$\lambda ex = 0.1019Pex+310.6 \quad (2)$$

Therefore, the EEM fluorometer spans excitation wavelengths in the region of 311 nm to 413 nm for this configuration.

CCD images of the reflected and scattered light show an approximately 5 nm bandpass for the excitation and emission spectra. The reflected/scattered spectral

images appear elliptical because the spectral range of the excitation (100 nm) and emission (60 nm) are not equal. The absence of cross-talk between the fibers in the coaxial array is evident in the CCD image of Rayleigh scattering from an aqueous starch suspension.

EEM spectra of pyrene (100 ppm), benzopyrene (100 ppm), and a binary mixture were collected with the coaxial fiber optic EEM fluorometer. The spectra of these two analytes lay within the spectral working range. Pyrene (Figure 11a) and benzopyrene (Figure 11b) were found to have excitation/emission maximum centers at approximately 337 nm – 362 nm/ 373 nm – 390 nm, and 310 nm – 412 nm/402 nm – 416 nm, respectively. For display purposes, the Rayleigh scattering has been truncated from the upper left corner of the image. The pyrene is less fluorescent than benzopyrene. The mixture spectra image could be distinguished in a binary mixture because the pure spectra images of pyrene and benzopyrene are not highly overlapped.

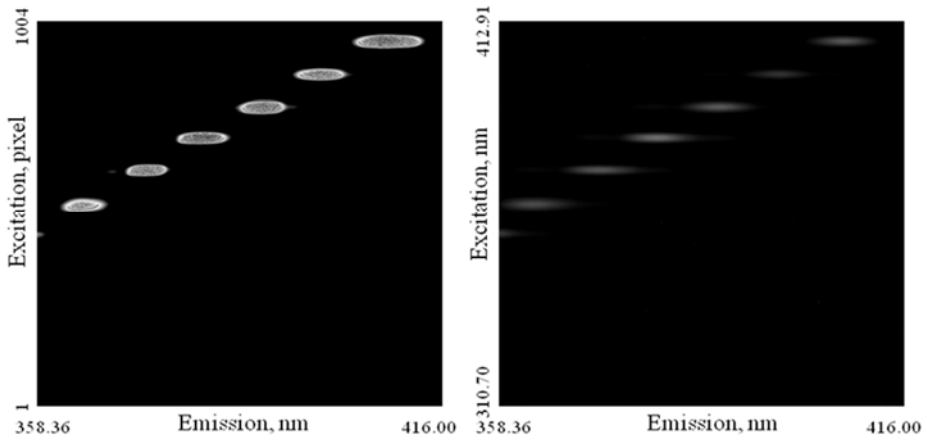

Figure 10. Reflected white light collected from a mirror (a) and Rayleigh scattering from a starch suspension (b) collected by the coaxial fiber optic EEM fluorometer was employed to calibrate the excitation spectrometer. The amount of cross-talk between the fibers in the array is insignificant.

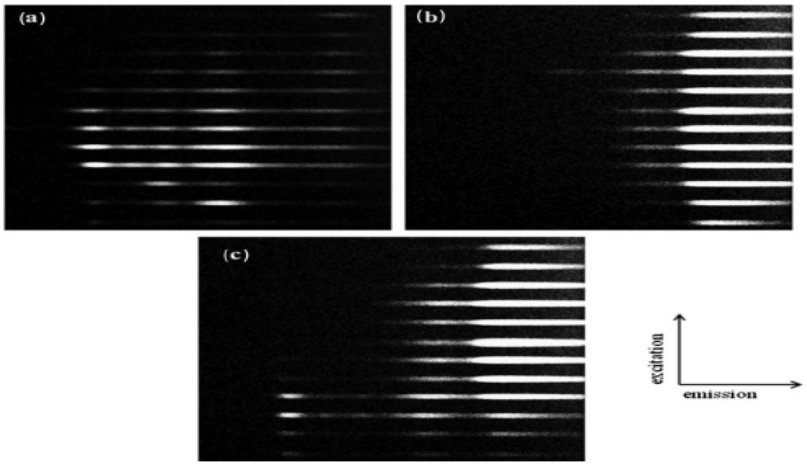

Figure 11. EEM spectra images of two PAHs and their mixture in the range 311–413 nm excitation and 358–416 nm emission. (a) Pyrene (100 ppm), (b) Benzopyrene (100 ppm), (c) Mixture of pyrene (100 ppm) and benzopyrene (100 ppm).

Evaluation of the equipment with cuvettes.

The inner fibers with the mercury-argon calibration source were used again to calibrate the emission spectrometer, which is shown in Figure 12, The five spots at each fiber are correlated with the known wavelengths (365.02, 365.48, 366.33, 404.66, 407.78 nm)7 and a linear polynomial fit is calculated to translate pixel numbers (from 115 to 860) into wavelengths in nm. The equation for the fitting line is:

$$\Delta\lambda em = 0.1932\Delta Pem + 274.65 \quad (1)$$

Where λem is the emission wavelength increase (nm) and Pem is the pixel number increase. The root mean square error (RMSE) of the calibration across the pixel range (121-187) is 0.9966. The CCD was set to detect the horizontal emission

wavelengths in the region of 274.65nm to 467.85nm. Therefore, the EEM fluorometer spans excitation wavelengths in the region of 286 nm to 378 nm for this configuration.

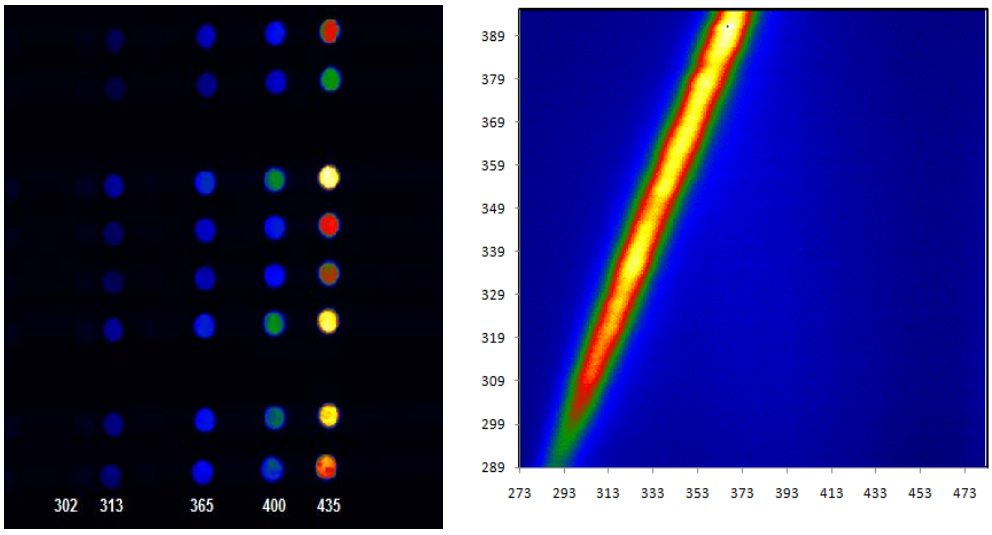

Figure 12. Calibration spectra a) for emission part, using a Hg lamp as source of light and b) for the excitation part using starch.

After calibration was done, a set of experiments were realized using different compounds pyrene, benzopyrene, benzopyrelene and a mixture of the three. The information obtained, shown in Fig. 13, can be further processed via PARAFAC, as determined previously by JiJi et al.[8],[11] to eliminate interferences from the EEM spectra. The results are shown in Fig. 14, and demonstrate that chemometrics tools can be used to advance the analysis of EEM data. This work was not further pursued.

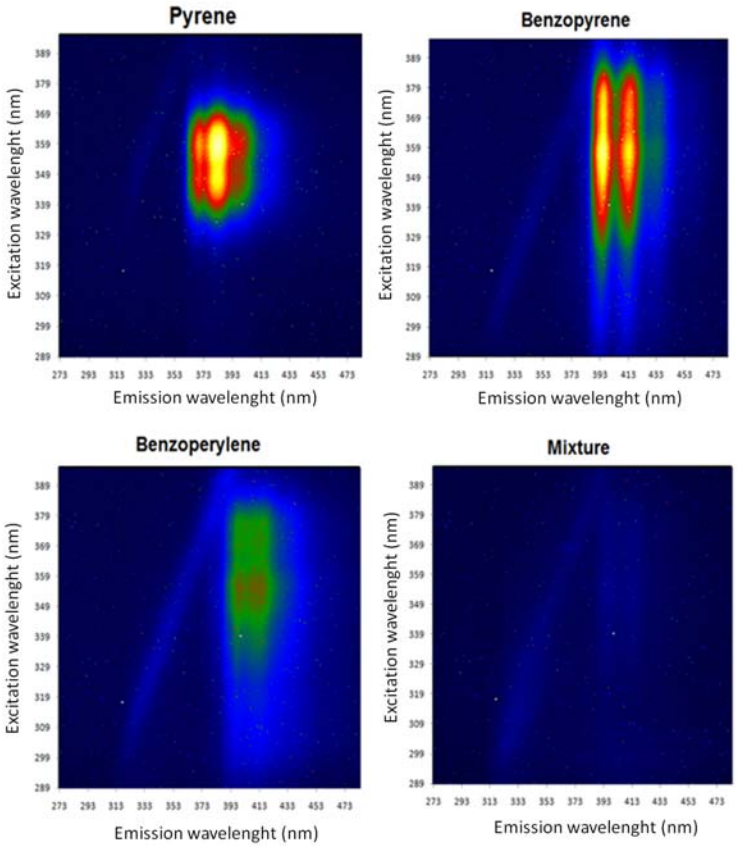

Figure 13. Representative EEM spectra for pure samples of 3 PAHs and a mixture of them. CCD temperature: -25 C; exposure time: 60 seconds. Concentrations in the ppb scale are employed in all cases.

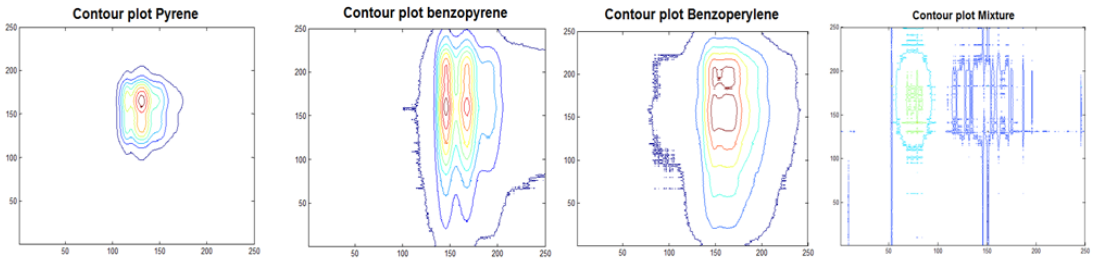

Figure 14. Reconstructed spectra obtained from the PARAFAC analysis. The background and the Rayleigh scattering contributions can be separated, leaving a "clean" EEM spectrum for the compounds.

Chapter 4

CONCLUSIONS

A novel design for detection of PAHs has been developed. The use of dispersive transmission (PGP) elements will be further exploited to build a portable fluorometer. The use of PARAFAC to process EEM data has been shown to offer significant advantages for the analysis of real samples. Future work can use this approach to analyze other compounds, such as pesticides.

In addition, a fiber optic excitation-emission matrix (EEM) fluorometer for PAH detection was developed. This method is based on the advanced modification of the geometry of the fiber optic EEM probe with coaxial design. This investigation indicates that the advanced probe geometry is promising for the development of fiber optic EEM fluorometer.

REFERENCES

1. Kim, Y. C., Jordan, J. A., Nahorniak, M. L. & Booksh, K. S. Photocatalytic degradation-excitation - Emission matrix fluorescence for increasing the selectivity of polycyclic aromatic hydrocarbon analyses. *Anal. Chem.* **77,** 7679–7686 (2005).

2. Gonul, L. T. & Kucuksezgin, F. Aliphatic and polycyclic aromatic hydrocarbons in the surface sediments from the Eastern Aegean: Assessment and source recognition of petroleum hydrocarbons. *Environ. Sci. Pollut. Res.* **19,** 31–41 (2012).

3. Manoli, E. & Samara, C. Polycyclic aromatic hydrocarbons in natural waters: Sources, occurrence and analysis. *TrAC - Trends Anal. Chem.* **18,** 417–428 (1999).

4. Rogers, S. W., Ong, S. K., Kjartanson, B. H., Golchin, J. & Stenback, G. A. Natural attenuation of polycyclic aromatic hydrocarbon-contaminated sites: Review. *Pract. Period. hazardous, toxic, Radioact. waste Manag.* **6,** 141–155 (2002).

5. Nahorniak, M. L., Cooper, G. A., Kim, Y.-C. & Booksh, K. S. Three-and four-way parallel factor (PARAFAC) analysis of photochemically induced excitation–emission kinetic fluorescence spectra. *Analyst* **140,** 85–93 (2005).

6. EPA. National Primary Drinking Water Regulations. 1–2 (1995).

7. Agency for Toxic Substances and Disease Registry (ATSDR). Toxicity of Polycyclic Aromatic Hydrocarbons (PAHs). *Case Stud. Environ. Med.* 1–68 (2009).

8. Jiji, R. D., Cooper, G. A. & Booksh, K. S. Excitation-emission matrix fluorescence based determination of carbamate pesticides and polycyclic aromatic hydrocarbons. *Anal. Chim. Acta* **397,** 61–72 (1999).

9. Muroski, A. R., Booksh, K. S. & Myrick, M. L. Single-Measurement Excitation/Emission Matrix Spectrofluorometer for Determination of Hydrocarbons in Ocean Water. 1. Instrumentation and Background Correction. *Anal. Chem.* **86,** 3539–3544 (1996).

10. Nahorniak, M. L. & Booksh, K. S. Excitation-emission matrix fluorescence spectroscopy in conjunction with multiway analysis for PAH detection in complex matrices. *Analyst* **131,** 1308 (2006).

11. Jiji, R. D., Andersson, G. G. & Booksh, K. S. Application of PARAFAC for calibration with excitation - Emission matrix fluorescence spectra of three classes of environmental pollutants. *J. Chemom.* **14,** 171–185 (2000).

12. Aikio, M. Hyperspectral prism-grating-prism imaging spectrograph. *VTT Publ.* 4–114 (2001).

13. Report, P. D., Shaffer, W., Sidoni, J., Scorse, D. & Gartenhaus, J. Hyperspectral Camera Design Project.

14. Cooney, T. F., Skinner, H. T. & Angel, S. M. Comparative study of some fiber-optic remote Raman probe designs. Part I: Model for liquids and transparent solids. *Appl. Spectrosc.* **50,** 849–860 (1996).

15. Ghandhi, J. B. Single- and dual-fiber fluorescence probes: application to oil-film measurements in an internal combustion engine. *Appl. Opt.* **39,** 5456–5464 (2000).

16. Ozanyan, K. B. *et al.* Fiber-based UV laser-diode fluorescence sensor for commercial gasolines. *IEEE Sens. J.* **4,** 681–690 (2004).

17. Wolf, B. a. Assay of cellular diacylglycerol and monoacylglycerol lipases. *Methods Mol. Biol.* **105,** 167–74 (1998).